ACS OMEGA

http://pubs.acs.org/journal/acsodf

Article

Mass-Transfer Simulation of Salicylic Acid on Weakly Polar Hyper-cross-linked Resin XDA-200 with Coadsorption of Sodium Ion

Pengfei Jiao,* Jiamiao Liu, Zhaoqi Wang, Maripat Ali, Luying Gu, and Shanshan Gao

Cite This: *ACS Omega* 2022, 7, 36679−36688

Read Online

ACCESS | Metrics & More | Article Recommendations | Supporting Information

ABSTRACT: The mass-transfer process of salicylic acid on hyper-cross-linked resin XDA-200 was experimentally and theoretically studied. Undissociated salicylic acid was found to be the favorable form for salicylic acid adsorption on the resin. A pH-dependent adsorption isotherm model established in this paper could well fit the adsorption isotherm data at different pH values. Surface diffusion is the main mass-transfer mode for salicylic acid in resin particles. The salicylate anions and Na^+ coadsorbed on the resin. The modified surface diffusion model considering the coadsorption was proposed. The model could satisfactorily fit the concentration decay curves of salicylic acid at different pH values and feed concentrations. NaOH aqueous solution at pH 12 could elute salicylic acid in the fixed bed efficiently. A pH-dependent dynamic adsorption and elution process model considering axial diffusion, external mass transfer, surface diffusion, pH-dependent adsorption equilibrium, as well as coadsorption of salicylate anions and Na^+ was established. The model could well predict the breakthrough and elution curves at different feed concentrations. The research carried out in this paper has reference significance for optimizing the separation process of salicylic acid and its analogues.

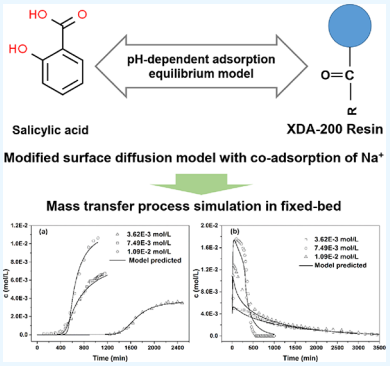

1. INTRODUCTION

The pollution of wastewater by drugs and their byproducts is an increasingly serious environmental problem.[1−3] Salicylic acid is one of the simplest aromatic phenolic acids.[4] It is a kind of analgesic, antipyretic drug and plays an important role in preventing platelet aggregation.[5] It is also an irreplaceable synthetic raw material for some traditional medicines such as aspirin and glyburide as well as a synthetic raw material or intermediate for food preservatives, dyes, and pesticides.[6] In recent years, salicylic acid has been identified as a water pollutant due to its chroma and high ecological toxicity.[7] Salicylic acid can be detected in sewage and even drinking water. It can impair liver and kidney function, cause protein degeneration, and even cause mucosal bleeding. The presence of salicylic acid in wastewater and drinking water is a global challenge.[8]

Many methods have been used to remove salicylic acid from wastewater, including extraction,[9] crystallization,[10] ozonation,[11] photocatalytic degradation,[12] membrane separation,[7] and adsorption.[13−15] However, each method has some disadvantages such as introduction of byproducts, complexity of process, ineffectiveness for treating low concentration target compound, and expensive operation costs.[16,17] Among the above methods, adsorption technology has become the most commonly used method for salicylic acid removal because of its advantages of convenient operation, simple equipment, high efficiency, low cost, and reusable adsorbents.[18,19] A series of adsorbents including hyper-cross-linked resins,[20−23] magnetic adsorption resin,[24] metal nanocomposites,[25] magnetic biochar,[14] and magnetic magnesium−zinc ferrites[26] have been prepared for the adsorption separation of salicylic acid. The adsorption thermodynamics and kinetics of salicylic acid have been studied in above studies. However, the simulation of mass-transfer process of salicylic acid in adsorbent particles and fixed bed has rarely been reported.

Mathematical modeling is a powerful tool for separation process design and optimization. Many mass-transfer models for adsorption separation process have been developed in the literature, such as solid-film linear-driving force model,[27] transport-dispersive model,[28] film−surface diffusion model,[29] general rate model, and so forth. Salicylic acid is a weak acid, and its dissociation degree is affected by solution pH. Therefore, the adsorption of salicylic acid depends on the solution pH and the dissociation equilibrium of salicylic acid. The cooperative adsorption of salicylate anions and metal ions in the solution is probably non-negligible. However, the coadsorption and dissociation equilibrium of adsorbates were rarely considered simultaneously in the mass-transfer simulation in the literature.

Hyper-cross-linked resins have many advantages such as large specific surface area, high adsorption capacity, high mechanical strength, and long service life.[30] Resins are the

Received: August 2, 2022
Accepted: September 30, 2022
Published: October 10, 2022

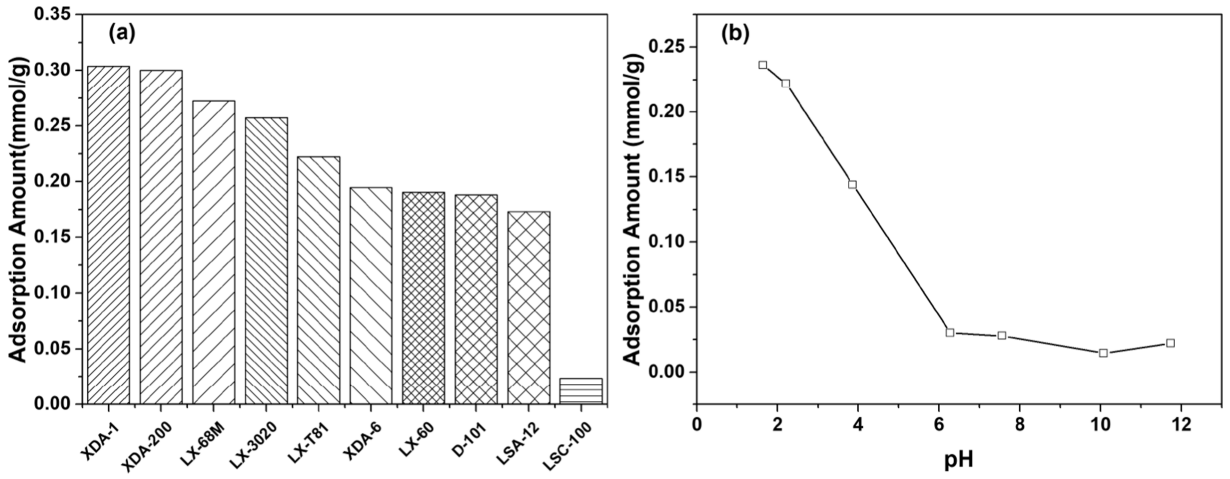

Figure 1. (a) Adsorption amounts of salicylic acid on different types of resins; (b) influence of pH on the adsorption capacity of XDA-200 resin.

most commonly used adsorbents for salicylic acid adsorption separation. Therefore, this work focused on the simulation of mass-transfer process of salicylic acid in hyper-cross-linked adsorption resin particles and fixed bed. First, the adsorption performances of salicylic acid on different types of resins were compared, and the resin with better performance was screened. Second, the rate-limiting step for mass transfer in the resin particles was studied by the intraparticle diffusion model, and the mass-transfer process in the particles was simulated considering the coadsorption of Na^+ and salicylate anions. Finally, the dynamic adsorption and desorption process of salicylic acid in the fixed bed were simulated. The studies carried out in this paper could provide a significant reference for optimizing the separation process of salicylic acid and its analogues.

2. RESULTS AND DISCUSSION

2.1. Screening the Resin for Salicylic Acid Adsorption. The adsorption capacities of salicylic acid on different types of hyper-cross-linked adsorption resins are shown in Figure 1a. The physicochemical properties of the resins are listed in Table 1. The adsorption capacities of XDA-200 and XDA-1 resins are higher than those of other resins (see Figure 1a). The result is probably due to the high specific surface area of above two resins. The specific surface area of resin XDA-200 is lower than those of resins LX-3020 and LX-68M. The high adsorption amount of resin XDA-200 may result from the fact that the carboxyl groups on the resin form hydrogen bond with salicylic acid molecules. High adsorption capacity is beneficial to improve the treatment capacity of feed solution and separation efficiency. However, resin XDA-1 is a nonpolar resin. The hydration of the resin is energetically unfavorable. Therefore, the resin is not suitable for aqueous adsorption systems. The adsorption capacity of resin XDA-200 to salicylic acid gradually decreases with increasing pH (see Figure 1b). When the pH values are relatively low, salicylic acid molecules mainly exist in an unionized form. As pH increases, the concentration ratio of salicylate anion increases. The solubility of the salicylate anion in water is greater than that of unionized salicylic acid, which leads to reduction of the adsorption capacity. When pH is higher than 5.0, the adsorption capacity of salicylic acid is close to 0, indicating that salicylic acid can be probably eluted from the resin efficiently when the pH of eluant is higher than 5.0. In conclusion, the XDA-200 resin was selected as the adsorbent for subsequent experiments.

Table 1. Physicochemical Properties of Resins Used in This Work

resin	matrix	S_{BET} (m^2/g)	polarity	functional group
XDA-200	PS-DVB[a]	1018.1	weakly polar	carbonyl
XDA-1	PS-DVB	1336.9	nonpolar	none
XDA-6	PS-DVB	673.5	nonpolar	none
LX-T81	PS-DVB	877.1	weakly polar	carbonyl
LX-3020	PS-DVB	1139	strongly polar	acylamide, ester group
LX-68M	PS-DVB	1082.1	weakly polar	ester group
LX-60	PS-DVB	845.1	weakly polar	ester group
LSC-100	PS-DVB	[b]	strongly polar	acylamide
LSA-12	PS-DVB	647	weakly polar	aldehyde group, carbonyl
D101	PS-DVB	728.8	weakly polar	carbonyl

[a]PS-DVB is the abbreviation of poly(styrene divinylbenzene). [b]The resin LSC-100 is a gel-type resin with a very low specific surface area.

The distribution coefficient of salicylic acid between solid and liquid phases under different pH conditions is shown in Figure 2. The values of the distribution coefficient decrease gradually with increasing pH, which is close to the change

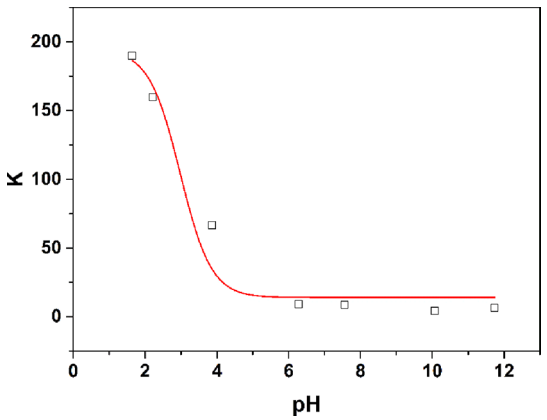

Figure 2. Influence of pH on the distribution coefficient of salicylic acid between solid and liquid phases.

https://doi.org/10.1021/acsomega.2c04892
ACS Omega 2022, 7, 36679−36688

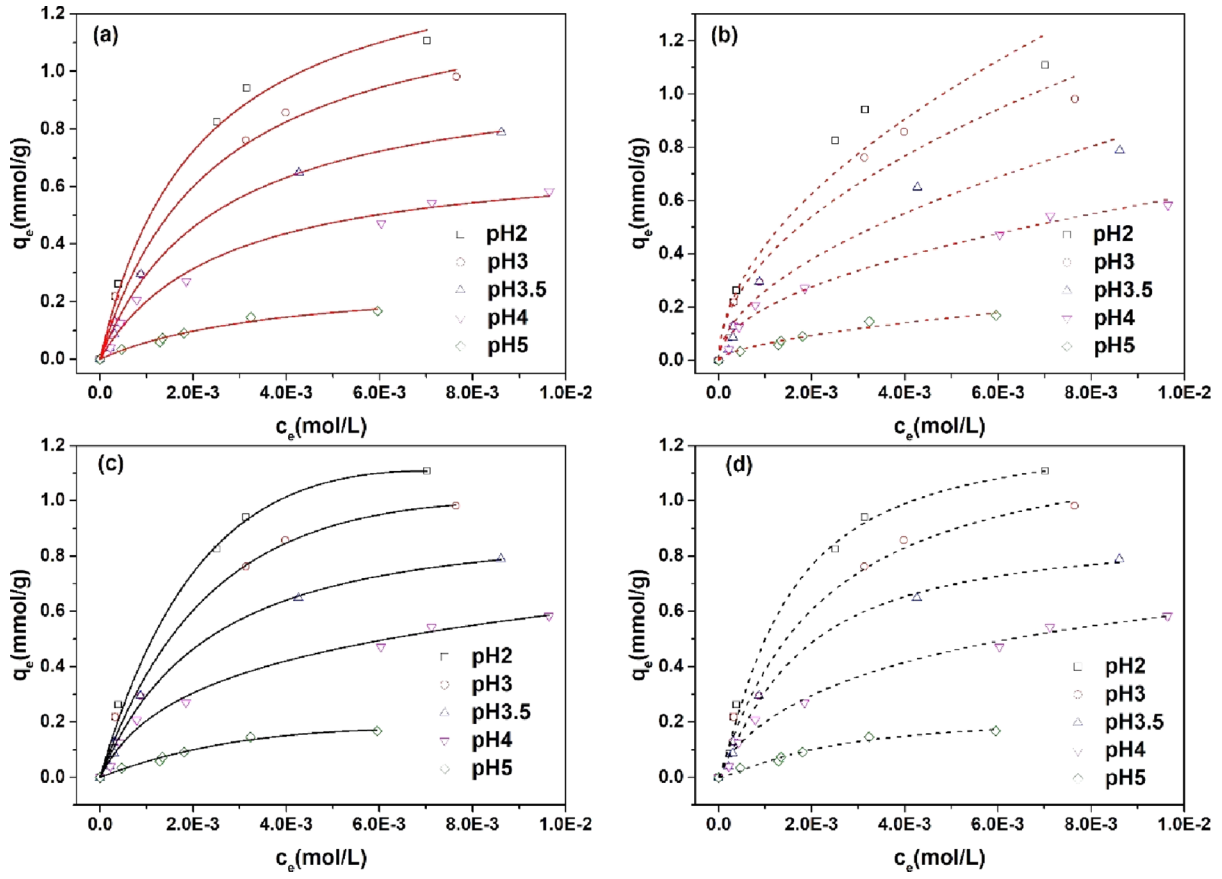

Figure 3. Experimental adsorption isotherms of salicylic acid and fitting results by (a) Langmuir model, (b) Freundlich model, (c) Toth model, and (d) Sips model.

Table 2. Adsorption Isotherm Model Parameters at Different pH Values

model parameters		pH 2.0	pH 3.0	pH 3.5	pH 4.0	pH 5.0
Langmuir model	q_m(mmol/g)	1.49	1.32	1.02	0.72	0.29
	k_L(L/mol)	470.89	413.90	410.97	389.47	256.07
	R^2	0.985	0.988	0.993	0.985	0.976
Freundlich model	k_f(L/mol)	17.40	12.70	10.98	6.09	3.74
	n	1.87	1.97	1.85	2.01	1.68
	R^2	0.934	0.958	0.961	0.984	0.956
Toth model	K_T(L/mol)	580.64	473.77	402.24	391.42	65.70
	α_T(L/mol)	107.32	157.50	313.18	1705.05	1.94×10^{-5}
	τ	0.43	0.61	0.88	1.54	1.40×10^{-7}
	R^2	0.989	0.988	0.992	0.989	0.980
Sips model	q_m(mmol/g)	1.25	1.26	0.89	1.01	0.22
	K_s(L/mol)	714.51	461.08	585.87	154.15	432.34
	n_s	1.25	1.06	1.19	0.75	1.32
	R^2	0.989	0.985	0.994	0.987	0.975

trend of the concentration ratio of nonionic salicylic acid in the solution. The results showed that nonionic salicylic acid was a favorable form for salicylic acid adsorption. The data in Figure 2 were fitted with the following empirical equation.[31]

$$K = \sum_{S} K_{S,d}\alpha_S \quad (1)$$

where K is the distribution coefficient of salicylic acid, S represents salicylic acid in different forms including nonionic salicylic acid and salicylate anion, and α_S represents the concentration ratio of salicylic acid in different forms.

The distribution coefficients of salicylic acid and salicylate anions obtained by fitting curves were 194.30 and 13.96, respectively. The distribution coefficient of nonionic salicylic acid was significantly higher than that of salicylate anion, indicating that the affinity between nonionic salicylic acid and resin was stronger than that between the salicylate anion and the resin.

2.2. Adsorption Equilibrium Behaviors of Salicylic Acid. Adsorption isotherms of salicylic acid on XDA-200 resin

https://doi.org/10.1021/acsomega.2c04892
ACS Omega 2022, 7, 36679−36688

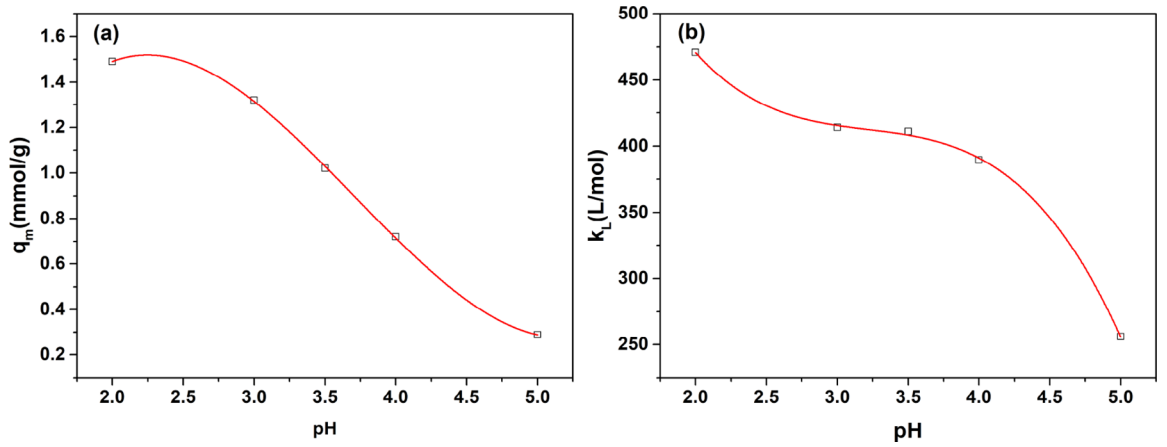

Figure 4. Variation curves of (a) q_m and (b) k_L values with solution pH.

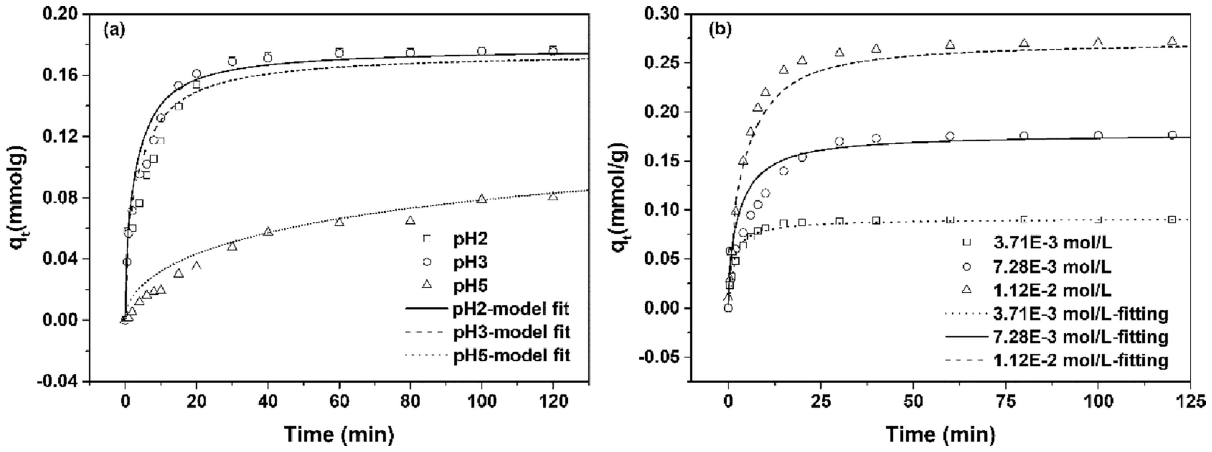

Figure 5. (a) Adsorption kinetics curves under different pH conditions; (b) adsorption kinetics curves under different initial concentrations.

under different pH conditions are shown in Figure 3. Langmuir, Freundlich, Toth, and Sips adsorption isotherm models were used to fit the adsorption isotherm data. The model parameters obtained by fitting curves are shown in Table 2. The values of correlation coefficient R^2 for Langmuir, Toth, and Sips models were close to each other. Moreover, the values of R^2 for the above three models were greater than or close to that of the Freundlich model. In order to simplify the model equation and calculation, Langmuir model was selected to describe the adsorption equilibrium behaviors of salicylic acid. All adsorption isotherms at different pH values are convex indicating that the adsorption of salicylic acid on the resin is favorable. All values of k_L are positive and decrease with increasing pH in the studies pH range. The k_L value is related to the adsorption strength. With the increase of pH, the affinity between salicylic acid and resin becomes weak, so k_L generally decreases with increasing pH. As can be seen from Figure 2, when the solution pH is higher than 5.0, the distribution coefficient barely changes. Therefore, the adsorption isotherms at pH values higher than 5.0 were considered the same as that at pH 5.0.

The changing curves of q_m and k_L with pH are shown in Figure 4a,b, respectively. The curves were fitted by several mathematical functions using nonlinear curve fitting in Origin 9.1. It was found that the following equation could well fit the curves.

$$q_m = -1.82 + 3.47\text{pH} - 1.11\text{pH}^2 + 0.1\text{pH}^3 \quad (2)$$

$$k_L = 1239.91 - 745.67\text{pH} + 227.72\text{pH}^2 - 23.59\text{pH}^3 \quad (3)$$

The fitting curves are shown in Figure 4a,b. The values of correlation coefficients of eqs 2 and 3 for fitting curves are 0.999 and 0.998, respectively. In conclusion, the pH-dependent adsorption isotherm model equation for salicylic acid is as follows

$$q_e = f(c_e, \text{pH}) \quad (4)$$

Ultimately, the adsorption equilibrium relationship of salicylic acid at different pH values can be predicted by above pH-dependent adsorption isotherm model.

2.3. Mass-Transfer Process of Salicylic Acid in Resin Particles. The adsorption kinetic curves for salicylic acid under different initial solution pH and concentration conditions are shown in Figure 5. As can be seen from Figure 5a, the adsorption amount at pH 5.0 is significantly lower than that at pH 2.0 and 3.0. The phenomenon can be explained by the fact that the concentration ratio of salicylate anion at pH 5.0 is higher than that at pH 2.0 and 3.0. The adsorption amount increases with increasing initial feed concentration (see Figure 5b). The result is consistent with that shown in Figure 3. The adsorption kinetics experimental data were fitted by the intraparticle diffusion model, and the fitting results are shown in Figure 6. The fitting results under different operating

https://doi.org/10.1021/acsomega.2c04892
ACS Omega 2022, 7, 36679−36688

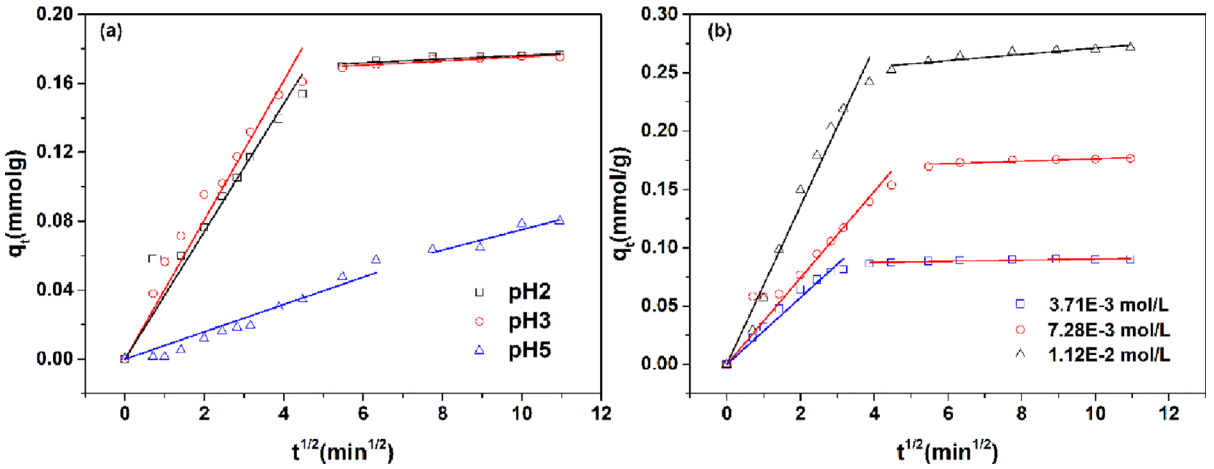

Figure 6. Intraparticle diffusion model fitting for the adsorption kinetics data of salicylic acid under different operating conditions: (a) Different initial pH; (b) different initial concentrations.

Table 3. Kinetic Adsorption Model Parameters for Salicylic Acid

	pH			initial concentration (mol/L)		
parameter	2	3	5	3.71×10^{-3}	7.28×10^{-3}	1.12×10^{-2}
D_s(cm^2/min)	5.0×10^{-7}	5.5×10^{-7}	5.3×10^{-7}	5.0×10^{-7}	5.0×10^{-7}	6.5×10^{-7}
ARD %	7.48	7.77	6.53	4.19	6.35	7.78

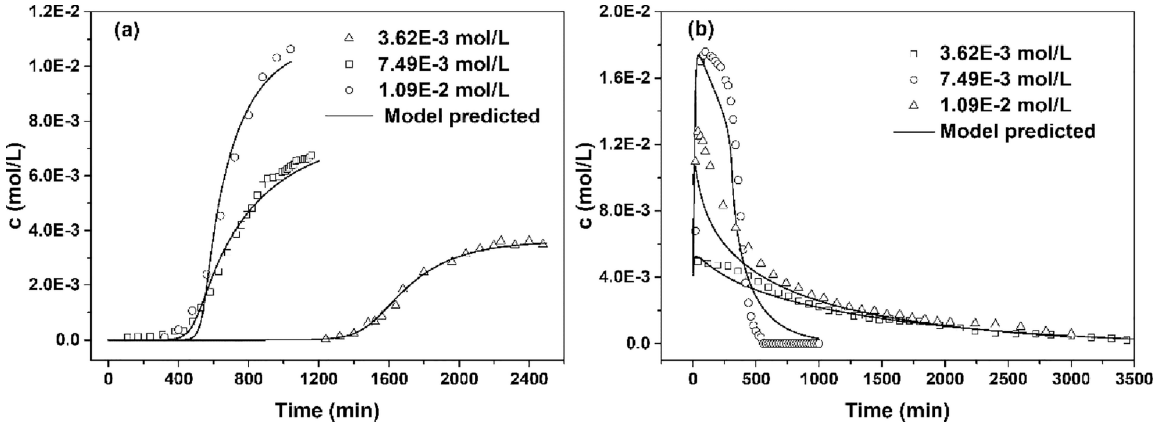

Figure 7. (a) Adsorption breakthrough curves of salicylic acid; (b) elution curves of salicylic acid.

conditions show a similar phenomenon, that is, each curve has two linear segments. In the first segment, the fitting lines all pass through the origin, indicating that intraparticle diffusion is the only rate-limiting step in the adsorption process of salicylic acid from the aqueous phase to the adsorption sites on the resin. A similar phenomenon was found in the adsorption process of rhodamine B on *N*-vinylimidazole-modified hyper-cross-linked resins.[32]

Sodium ions do not adsorb on the XDA-200 resin. However, coadsorption exists between Na^+ and salicylate anions due to electrostatic attraction. The change of Na^+ concentration in solution will lead to the change of solution pH, thus affecting the adsorption of salicylic acid. In order to verify the existence of coadsorption, both the modified surface diffusion model with coadsorption and that without coadsorption were used to fit the adsorption kinetics data under different pH conditions. The fitting results are shown in Figures 5a and S1. As can be seen from Figures 5a and S1, when the solution pH is ∼2 and 5, the fitting results of the two models are not significantly different. However, there is a significant difference between the simulated curve in Figure S1 and the experimental data when the solution pH is ∼3. At pH 2, there is no Na^+ in the solution. Therefore, coadsorption does not exist. When pH is ∼5, the concentration of Na^+ in the solution is relatively high, while the adsorption capacity of salicylic acid is relatively low. Therefore, the amount of Na^+ adsorbed on the resin via coadsorption with salicylate anions is small relative to the amount of Na^+ in the solution, which has no significant influence on the solution pH and the adsorption amount of salicylic acid. When the solution pH is ∼3, the concentration of Na^+ in the solution is relatively low, and the amount of Na^+ adsorbed on the resin is relatively large, resulting in a significant change in solution pH. Therefore, the fitting results of the model without considering the coadsorption of Na^+ differ greatly from the experimental results. In sum, the coadsorption of Na^+ with salicylate anions is negligible at about pH 3.0.

The modified surface diffusion model with coadsorption of Na^+ and salicylate anions was used to fit the adsorption kinetic

https://doi.org/10.1021/acsomega.2c04892
ACS Omega 2022, 7, 36679−36688

curves of salicylic acid under different pH and concentration conditions, and the fitting curves are shown in Figure 5. The values of model parameters obtained by fitting are listed in Table 3. The values of ARD % are all lower than 8.0%, indicating that the model can provide a general prediction to the adsorption kinetics data. The results show that the mass-transfer process of salicylic acid in XDA-200 resin particles can be well simulated by the modified surface diffusion model. For microporous adsorbents, surface diffusion is the main mass-transfer mode for adsorbates in adsorbent pores. Therefore, the model is suitable for salicylic acid adsorption in XDA-200 resin with a pronounced micropore system.

2.4. Dynamic Adsorption and Elution of Salicylic Acid. The adsorption breakthrough and elution curves of salicylic acid are shown in Figure 7a,b, respectively. As can be seen from Figure 7a, the stoichiometric time ($c_t = 0.5c_{fe}$) of salicylic acid decreases with increasing initial concentration of the feed solution. This is because the adsorption isotherms of salicylic acid are convex. For convex isotherms, the retention time of adsorbates decreases with increasing concentration.[33] The elution yields of salicylic acid were all higher than 99%. When the initial concentrations of the feed solution were 3.62×10^{-2} and 1.09×10^{-2} mol/L, deionized water was used as the eluant. The elution curves tailed severely. Nearly 3000 min was needed to elute salicylic acid completely (see Figure 7b). When the initial concentration was 7.49×10^{-2} mol/L, the salicylic acid could be eluted quickly with NaOH aqueous solution at pH 12 used as the eluant (eluting time was less than 500 min). The rapid elution of salicylic acid was due to the rapid increase of pH of the mobile phase in the chromatographic column, which leads to the fact that salicylic acid mainly exists in the form of anions. The weak affinity between salicylate anions and resin results in the rapid outflow of salicylic acid from the chromatographic column. The breakthrough and elution curves of salicylic acid predicted by the pH-dependent dynamic separation process model proposed in this paper are shown in Figure 7. The values of model parameters are shown in Table S1. As can be seen from Figure 7, the model can well predict the breakthrough and elution curves of salicylic acid at different initial concentrations of the feed solution. The results indicate that the model proposed in this paper can be used to simulate the mass-transfer process of salicylic acid and further optimize the separation process.

3. CONCLUSIONS

The mass-transfer process of salicylic acid on weakly polar hyper-cross-linked resin XDA-200 was experimentally and theoretically studied. The pH-dependent adsorption isotherm model proposed in this paper can well fit the adsorption isotherms of salicylic acid under different pH conditions. Surface diffusion is the main mass-transfer mode of salicylic acid in XDA-200 resin particles. The coadsorption of Na^+ and salicylate anions exists in the adsorption system. The modified surface diffusion model considering the coadsorption can well fit the adsorption kinetics curves of salicylic acid under different pHs and initial solution concentrations. The dynamic separation process model considering the dissociation equilibrium of salicylic acid and coadsorption of Na^+ and salicylate anions was established in this paper. The model can well predict the mass-transfer process of salicylic acid in fixed -bed with various feed concentrations and pH values. The research carried out in this paper has a certain reference significance for the efficient separation of salicylic acid and its analogues.

4. MATERIALS AND METHODS

4.1. Resins. The hyper-cross-linked resins used in this paper were purchased from Sunresin New Materials Co., Ltd., Xi'An (Xi'An, China). The pretreatment methods of the resins can be found in our previous paper.[34]

4.2. Chemicals. Salicylic acid and hydrochloric acid were purchased from Tianjin Hengxing Chemical Reagent Manufacturing Co., Ltd. (Tianjin, China). Sodium hydroxide and anhydrous ethanol were provided by Tianjin Fengchuan Chemical Reagent Technology Co., Ltd. (Tianjin, China) and Wuxi Yatai United Chemical Co., Ltd. (Wuxi, China), respectively. All above reagents were of analytical grade and used without further purification. Deionized water was prepared by a laboratory pure water machine (WP-UP-YJ-40, Sichuan Wortel Water Treatment Equipment Co., Ltd., Chengdu, China).

4.3. Screening Resin for Salicylic Acid Adsorption and Determination of Adsorption Isotherms of Salicylic Acid. An aqueous solution of salicylic acid (~3.62×10^{-3} mol/L) was prepared from which 25 mL was taken out and put into several 50 mL triangular bottles. Then XDA-200 resin (1 g) was added to each triangle flask. The adsorption equilibrium was achieved by shaking the flasks at 150 rpm and 298 ± 1 K in a shaker (HNY-200B, Tianjin Honour Instrument Co., Ltd., Tianjin, China) for more than 5 h. The concentration of salicylic acid was measured at 296 nm by an UV−vis spectrophotometer (BioSpectrometer, Eppendorf AG, Hamburg, Germany). The adsorption capacity of salicylic acid was calculated according to eq 5.

$$q_e = \frac{V \times (c_0 - c_e)}{M} \tag{5}$$

where q_e is the adsorption capacity of salicylic acid (mmol/g), c_0 is the concentration of solution before adsorption (mol/L), c_e is the concentration of solution at adsorption equilibrium (mol/L), V is the volume of solution (mL), and M is the mass of resin (g).

The adsorption capacities of other resins were determined by a procedure similar to that of XDA-200 resin. The adsorption capacities of the resins were compared to select the adsorbent for subsequent experiments.

An aqueous solution of salicylic acid (~3.62×10^{-3} mol/L) was prepared. 50 mL of the solution was taken out and placed in several 100 mL triangle flasks. The solutions were adjusted to different pH values (1.5, 2.0, 2.5, 8.0, 9.0, 11.0, and 12.0). Then, the wet resin XDA-200 (0.5 g) was added to the flasks. The flasks were shaken at 150 rpm and 298 ± 1 K in a shaker for more than 5 h to achieve adsorption equilibrium. The pH values of the solutions were determined by a pH meter (FE28, Mettler-Toledo, LLC, Zurich, Switzerland), and the concentration of salicylic acid was measured. The adsorption capacity of salicylic acid was calculated according to eq 5.

Several aqueous solutions of salicylic acid at different concentrations were prepared. 25 mL of the solutions was taken and placed in several 50 mL triangulated bottles. Then, the wet resin XDA-200 (2 g) was added to each bottle. The pH of the solutions was adjusted to 2.0. The adsorption equilibrium was achieved using the same procedures as above. The adsorption capacity at different initial concentrations was

https://doi.org/10.1021/acsomega.2c04892
ACS Omega 2022, 7, 36679−36688

determined. The changing curve of adsorption capacity with equilibrium concentration was the adsorption isotherm at pH 2.0. The adsorption isotherms under other pH conditions were determined by similar procedures.

4.4. Adsorption Kinetics Curves at Different Initial pH Values and Concentrations. The aqueous solution of salicylic acid (250 mL) at a concentration of ~7.24×10^{-3} mol/L was prepared and placed in a 500 mL round-bottom flask. The solution pH was adjusted to ~2.0. Then, the wet resin XDA-200 (10 g) was added into the flask. The mixture was stirred vigorously, and several samples were taken at different time intervals to determine the concentration of salicylic acid. Equation 5 was used to calculate the adsorption capacity of salicylic acid at different moments. The adsorption kinetics curve at pH 2.0 was prepared with time as abscissa and adsorption capacity at different moments as the ordinate. Then, the adsorption kinetics curves at pH 3 and 5 and those at different initial concentrations were measured by the same method.

4.5. Dynamic Adsorption and Elution Curves of Salicylic Acid. Hydrochloric acid solution at pH 2.0 was passed into a glass chromatographic column of 1.15 cm inner diameter from the upper end of the column. The column was filled with resin XDA-200 (3 g). A pH meter was used to measure the pH values of the effluent at the exit of the column until the pH value approaches 2.0. Then, the salicylic acid aqueous solution (~7.24×10^{-3} mol/L) was prepared, and the pH value was adjusted to 2.0. The solution was passed into the chromatographic column through the upper end. A peristaltic pump (BT100-1L, Hebei, China) was used to control the flow rate at 0.5 mL/min. A partial collector was used to collect samples at the exit of the column at regular intervals and to determine the concentration of the samples. The injection was finished until the solution concentration at the exit of the column was close to the concentration of the feed solution. The curve of the solution concentration at the exit of the column over time was the breakthrough curve of salicylic acid. After the injection was finished, the column was eluted with NaOH solution at pH 12 at a flow rate of 0.5 mL/min until the solution concentration approached 0. The elution curve of salicylic acid was the changing curve of the solution concentration at the outlet of the column with time. The breakthrough and elution curves at other initial concentrations of feed solution were determined using the same operation method except that deionized water was used as the eluant.

All experiments in this paper were carried out at least 3 times with an experimental error of less than 6%. The data listed in this paper are the average values of three groups of experimental data.

5. THEORY

5.1. Adsorption Isotherm Models. *5.1.1. Langmuir Adsorption Isotherm Model.*

$$q_e = \frac{q_m k_L c_e}{1 + k_L c_e} \tag{6}$$

where q_m is the maximum monolayer adsorption capacity (mmol/g) and k_L is Langmuir constant (L/mol).

5.1.2. Freundlich Adsorption Isotherm Model.

$$q_e = k_f c_e^{1/n} \tag{7}$$

where k_f and n are Freundlich constants.

5.1.3. Toth Isotherm Model.[35]

$$q_e = \frac{K_T c_e}{(1 + \alpha_T c_e)^{1/\tau}} \tag{8}$$

where K_T (L/mol), α_T (L/mol), and τ are constants of the Toth isotherm model.

5.1.4. Sips Adsorption Isotherm Model.

$$q_e = \frac{q_m (K_s c_e)^{n_s}}{1 + (K_s c_e)^{n_s}} \tag{9}$$

where K_s presents the adsorption energy (L/mol) and n_s is the heterogeneity factor.

5.2. Kinetic Adsorption Models. *5.2.1. Intraparticle Diffusion Model.* Intraparticle diffusion model proposed by Weber and Morris can be described by the following equation[36]

$$q_t = k_p t^{1/2} \tag{10}$$

where q_t is the adsorption amount at time t (mmol/g), k_p is the diffusion rate parameter [(mmol/g)/(min)$^{1/2}$], and t is the time (min).

5.2.2. Modified Surface Diffusion Model. In order to simplify the model, the following model assumptions were made. The temperature of the adsorption system remained constant during the adsorption process. The adsorbent was spherical particles of uniform size. The radial solute concentration distribution in the column was uniform.

Modified surface diffusion model contains the following equations.

The mass conservation equations of salicylic acid and Na^+ between solid and liquid phases are as follows

$$-V \frac{dc_{SA,b}}{dt} = M \int_0^R q_t \, dr \tag{11}$$

$$-V \frac{dc_{Na^+}}{dt} = M \int_0^R q_t \frac{K_e}{c_{H^+} + K_e} \, dr \tag{12}$$

where $c_{SA,b}$ is the concentration of salicylic acid in the bulk solution (mol/L). R is the radius of resin particles (cm). r is the radial position within resin particles (cm). c_{Na^+} and c_{H^+} are the concentrations of Na^+ and H^+ in the bulk solution (mol/L).

The mass conservation equation of salicylic acid in the resin particle element is as follows

$$\frac{\partial q_t}{\partial t} = \frac{D_s}{r^2} \frac{\partial}{\partial r} \left(r^2 \frac{\partial q_t}{\partial r} \right) \tag{13}$$

where D_s is the surface diffusion coefficient (cm^2/min).

In the aqueous solution, the dissociation degree of salicylic acid depends on the solution pH. The dissociation process of salicylic acid is shown as follows

$$SA \xrightarrow{K_e} SA^- + H^+ \tag{14}$$

where K_e is the dissociation equilibrium constant of salicylic acid and its value is 1.05×10^{-3}.[37] The second dissociation equilibrium constant of salicylic acid (2.19×10^{-14}) was neglected in this paper. SA represents unionized salicylic acid. SA^- represents the anionic form of salicylic acid. The calculation equations of the concentration of salicylic acid in different forms are as follows

https://doi.org/10.1021/acsomega.2c04892
ACS Omega 2022, 7, 36679−36688

$$c_{SA} = \frac{c_{SA,b} c_{H^+}}{c_{H^+} + K_e} \quad (15)$$

$$c_{SA^-} = \frac{c_{SA,b} K_e}{c_{H^+} + K_e} \quad (16)$$

where c_{SA} and c_{SA^-} are the concentrations of unionized salicylic acid and salicylate anion, respectively (mol/L).

The electroneutral condition in the solution is as follows

$$c_{H^+} + c_{Na^+} - c_{SA^-} - c_{Cl^-} - c_{OH^-} = 0 \quad (17)$$

where c_{Cl^-} and c_{OH^-} are the concentrations of Cl^- and OH^-, respectively (mol/L).

The values of c_{H^+} and c_{OH^-} can be related by the following equation

$$c_{H^+} \times c_{OH^-} = 10^{-14} \quad (18)$$

The pH values can be calculated using the following equation

$$pH = -\log_{10} c_{H^+} \quad (19)$$

The initial and boundary conditions are shown below

$$t = 0 \qquad q_0 = 0 \qquad c_{SA,b} = c_{SA,fe} \quad (20)$$

$$r = 0 \qquad \frac{\partial q_t}{\partial r} = 0 \quad (21)$$

$$r = R \qquad q_t(R) = f(c_{SA,b}, pH) \quad (22)$$

where $c_{SA,fe}$ is the concentration of salicylic acid in the feed solution (mol/L).

The concentration history in bulk solution and the concentration profiles in resin particles can be obtained by solving the above equations using MATLAB2010a. The partial differential equations were discretized into ordinary differential equations by the orthogonal configuration finite element method. Then, the ordinary differential equations were solved by ODE23. The relative and absolute tolerances are 10^{-5}. The values of D_s are solved by minimizing the following objective function

$$\text{Minimum} = \sum_{j=1}^{N} \left(\frac{c_{j,exp} - c_{j,pred}}{c_{j,exp}} \right)^2 \quad (23)$$

where N is the number of experimental data points. $c_{j,exp}$ and $c_{j,pred}$ are the experimentally measured and predicted concentrations of salicylic acid, respectively (mol/L).

The average relative deviation between the experimentally measured and predicted adsorption kinetics data can be expressed by the following equation

$$ARD\ \% = \frac{1}{N} \sum_{j=1}^{N} \left| \frac{c_{j,exp} - c_{j,pred}}{c_{j,exp}} \right| \times 100 \quad (24)$$

5.3. Dynamic Separation Process Model in the Chromatographic Column. Axial diffusion and liquid film mass transfer were considered in this model.

The mass conservation equation of salicylic acid in the axial mobile phase of fixed bed is as follows

$$v \frac{\partial c_i}{\partial x} + \frac{\partial c_i}{\partial t} + \frac{1 - \varepsilon_b}{\varepsilon_b} \frac{3}{R} k_{i,film}(c_i - c_{i,s}) = D_{ax} \frac{\partial^2 c_i}{\partial x^2} \quad (25)$$

where v is the interstitial velocity (cm/min), c_i and $c_{i,s}$ are the concentration of solute i in the mobile phase and near the surface of the resin particles, respectively (mol/L), x is the axial position in the fixed bed (cm), ε_b is the bed voidage, $k_{i,film}$ is the diffusion coefficient in the liquid film outside of the resin particles (cm/min), and D_{ax} are axial diffusion coefficients (cm^2/min).

The mass conservation equations of Na^+ and Cl^- in the axial mobile phase of fixed bed are as follows

$$v \frac{\partial c_{Na^+}}{\partial x} + \frac{\partial c_{Na^+}}{\partial t} = D_{Na^+,ax} \frac{\partial^2 c_{Na^+}}{\partial x^2} - \frac{1 - \varepsilon_b}{\varepsilon_b} \frac{3}{R} \rho_p D_s \left. \frac{dq_{SA}}{dr} \right|_{r=R} \frac{K_e}{c_{H^+} + K_e} \quad (26)$$

$$v \frac{\partial c_{Cl^-}}{\partial x} + \frac{\partial c_{Cl^-}}{\partial t} = D_{Cl^-,ax} \frac{\partial^2 c_{Cl^-}}{\partial x^2} \quad (27)$$

ρ_p is the apparent wet density of the resin (g/mL).

The mass-transfer process of salicylic acid in resin particles is expressed by eq 13.

The boundary conditions of fixed bed and resin particles are as follows

$$x = 0\ (\text{inlet}),\ t > 0 \qquad D_{i,ax} \frac{\partial c_i}{\partial x} = v(c_i|_{x=0} - c_{i,in}) \quad (28)$$

$$x = L_c\ (\text{outlet}),\ t > 0 \qquad \left. \frac{\partial c_i}{\partial x} \right|_{x=L_c} = 0 \quad (29)$$

$$r = 0 \qquad \frac{\partial q_{SA}}{\partial r} = 0 \quad (30)$$

$$r = R \qquad D_{SA,s} \frac{\partial q_{SA}}{\partial r}|_{r=R} = \frac{k_{SA,film}}{\rho_p}(c_{SA} - c_{SA,s}) \quad (31)$$

The initial conditions during adsorption are as follows

$$c_i = 0;\ q_i = 0 \quad (32)$$

The concentration and adsorption capacity of adsorbates in the column at the end of the adsorption stage are the initial conditions during desorption.

The adsorption equilibrium of salicylic acid molecules on the surface of resin particles is reached instantaneously. The adsorption equilibrium equation is expressed as follows

$$q_{SA}(R) = f(c_{SA,s}, pH) \quad (33)$$

Equations 14−17 were used to calculate the concentrations of salicylic acid in different dissociation states in the mobile phase and express the electric neutral conditions.

The solving method of the above model equations is similar to that of the modified surface diffusion model.

$D_{i,ax}$ and $k_{i,film}$ were calculated using the following equations[38]

$$D_{i,ax} = 0.44 D_{i,m} + 0.83 U d_p \quad (34)$$

$$k_{i,film} = \frac{1.09}{\varepsilon_b} \frac{D_{i,m}}{d_p} \left(\frac{v \cdot d_p}{D_{i,m}} \right)^{1/3} \quad (35)$$

https://doi.org/10.1021/acsomega.2c04892
ACS Omega 2022, 7, 36679−36688

where U is the superficial velocity of the mobile phase (cm/min), d_p is the diameter of the resin particles (cm), and $D_{i,m}$ is the molecular diffusivity of solute i (cm^2/min). The values of $D_{Na^+,m}$ and $D_{Cl^-,m}$ are 7.8×10^{-4} and 1.79×10^{-3} cm^2/min, respectively.[39,40] The value of $D_{SA,m}$ was calculated by Wilke–Chang correlation as follows.[41]

$$D_{i,m} = \frac{7.4 \times 10^{-8}(\phi M_B)^{1/2} T}{\eta_B V_{i,A}^{0.6}} \quad (36)$$

where φ is the association parameter, M_B is the molecular weight of water, T is the operating temperature (K), η_B is the viscosity of the solution (mPa·s), and $V_{i,A}$ is molar volume of adsorbate i at its normal boiling point [mL/(g·mol)].

■ ASSOCIATED CONTENT

Supporting Information

The Supporting Information is available free of charge at https://pubs.acs.org/doi/10.1021/acsomega.2c04892.

Adsorption kinetics curves of salicylic acid on XDA-200 resin predicted by the modified surface diffusion model without coadsorption of Na^+ and operating and model parameters for salicylic acid (PDF)

■ AUTHOR INFORMATION

Corresponding Author

Pengfei Jiao − *Research Center of Henan Provincial Agricultural Biomass Resource Engineering and Technology, College of Life Science and Agricultural Engineering, Nanyang Normal University, Nanyang 473061, China;* orcid.org/0000-0001-6918-2162; Phone: +86-0377-63513605; Email: jiaopf126@126.com; Fax: +86-0377-63512517

Authors

Jiamiao Liu − *Research Center of Henan Provincial Agricultural Biomass Resource Engineering and Technology, College of Life Science and Agricultural Engineering, Nanyang Normal University, Nanyang 473061, China*

Zhaoqi Wang − *Research Center of Henan Provincial Agricultural Biomass Resource Engineering and Technology, College of Life Science and Agricultural Engineering, Nanyang Normal University, Nanyang 473061, China*

Maripat Ali − *Research Center of Henan Provincial Agricultural Biomass Resource Engineering and Technology, College of Life Science and Agricultural Engineering, Nanyang Normal University, Nanyang 473061, China*

Luying Gu − *Research Center of Henan Provincial Agricultural Biomass Resource Engineering and Technology, College of Life Science and Agricultural Engineering, Nanyang Normal University, Nanyang 473061, China*

Shanshan Gao − *Research Center of Henan Provincial Agricultural Biomass Resource Engineering and Technology, College of Life Science and Agricultural Engineering, Nanyang Normal University, Nanyang 473061, China*

Complete contact information is available at: https://pubs.acs.org/10.1021/acsomega.2c04892

Notes

The authors declare no competing financial interest.

■ ACKNOWLEDGMENTS

This research was supported by the Scientific and Technological Project of Henan Province (grant no. 202102110285) and School-Level Research Project of Nanyang Normal University (grant no. 2018ZX009).

■ REFERENCES

(1) Bessergenev, V. G.; Mateus, M. C.; Morgado, I. M.; Hantusch, M.; Burkel, E. Photocatalytic reactor, CVD technology of its preparation and water purification from pharmaceutical drugs and agricultural pesticides. *Chem. Eng. J.* **2017**, *312*, 306−316.

(2) Brumovský, M.; Bečanová, J.; Kohoutek, J.; Borghini, M.; Nizzetto, L. Contaminants of emerging concern in the open sea waters of the Western Mediterranean. *Environ. Pollut.* **2017**, *229*, 976−983.

(3) Dordio, A. V.; Miranda, S.; Prates Ramalho, J. P.; Carvalho, A. P. Mechanisms of removal of three widespread pharmaceuticals by two clay materials. *J. Hazard. Mater.* **2017**, *323*, 575−583.

(4) Meng, X.; Liu, T.; Huo, S.; Wang, L. Separation of salicylic acid and two phenols by polyvinyl chloride/N,N-bis (1-methylheptyl) acetamide polymer inclusion membrane. *J. Water Process. Eng.* **2021**, *41*, 102015−102022.

(5) Taoufik, N.; Elmchaouri, A.; El Mahmoudi, S. E.; Korili, S. A.; Gil, A. Comparative Analysis Study by Response Surface Methodology and Artificial Neural Network on Salicylic Acid Adsorption Optimization using Activated Carbon. *Environ. Nanotechnol., Monit. Manage.* **2021**, *15*, 100448−100457.

(6) Mark, R.; Lyu, X.; Lee, J.; Parra-Saldívar, R.; Chen, W. N. Sustainable production of natural phenolics for functional food applications. *J. Funct. Foods* **2019**, *57*, 233−254.

(7) Yu, X.; Mi, X.; He, Z.; Meng, M.; Li, H.; Yan, Y. Fouling Resistant CA/PVA/TiO2 Imprinted Membranes for Selective Recognition and Separation Salicylic Acid from Waste Water. *Front. Chem.* **2017**, *5*, 2−14.

(8) Santamaría, L.; Vicente, M. A.; Korili, S. A.; Gil, A. Effect of the preparation method and metal content on the synthesis of metal modified titanium oxide used for the removal of salicylic acid under UV light. *Environ. Technol.* **2020**, *41*, 2073−2084.

(9) Haensel, R.; Halwachs, W.; Schügerl, K. Physical and reactive extraction of salicylic acid—I. Thermodynamic and kinetic investigations in a stirred cell. *Chem. Eng. Sci.* **1986**, *41*, 135−141.

(10) Caro, J. A.; Woldehaimanot, M.; Rasmuson, Å. C. Semibatch reaction crystallization of salicylic acid. *Chem. Eng. Res. Des.* **2014**, *92*, 522−533.

(11) Vel Leitner, N. K.; Delouane, B.; Legube, B.; Luck, F. Effects of catalysts during ozonation of salicylic acid, peptides and humic substances in aqueous solution. *Ozone: Sci. Eng.* **1999**, *21*, 261−276.

(12) Ozyonar, F. Removal of Salicylic Acid from Aqueous Solutions Using Various Electrodes and Different Connection Modes by Electrocoagulation. *Int. J. Electrochem. Sci.* **2016**, *11*, 3680−3696.

(13) Fu, Z.; Huang, J. Polar hyper-cross-linked resin with abundant micropores/mesopores and its enhanced adsorption toward salicylic acid: Equilibrium, kinetics, and dynamic operation. *Fluid Phase Equilib.* **2017**, *438*, 1−9.

(14) Karunanayake, A. G.; Todd, O. A.; Crowley, M. L.; Ricchetti, L. B.; Pittman, C. U.; Anderson, R.; Mlsna, T. E. Rapid removal of salicylic acid, 4-nitroaniline, benzoic acid and phthalic acid from wastewater using magnetized fast pyrolysis biochar from waste Douglas fir. *Chem. Eng. J.* **2017**, *319*, 75−88.

(15) Chen, G.; Zeng, X.; Huang, J. Imidazole-modified polymers and their adsorption of salicylic acid from aqueous solution. *J. Polym. Res.* **2022**, *29*, 1−7.

(16) Escapa, C.; Coimbra, R. N.; Paniagua, S.; García, A. I.; Otero, M. Paracetamol and salicylic acid removal from contaminated water by microalgae. *J. Environ. Manage.* **2017**, *203*, 799−806.

(17) Kyzas, G. Z.; Fu, J.; Lazaridis, N. K.; Bikiaris, D. N. New approaches on the removal of pharmaceuticals from wastewaters with adsorbent materials. *J. Mol. Liq.* **2015**, *209*, 87−93.

https://doi.org/10.1021/acsomega.2c04892
ACS Omega 2022, 7, 36679−36688

(18) Smiljanić, D.; Dakovi, A.; Obradovi, M.; Oegovi, M.; Izzo, F.; Germinario, C.; Gennaro, B. D. Application of Surfactant Modified Natural Zeolites for the Removal of Salicylic Acid—A Contaminant of Emerging Concern. *Materials* **2021**, *14*, 7728.
(19) Lee, X. J.; Chemmangattuvalappil, N.; Lee, L. Y. Adsorptive removal of salicylic acid from aqueous solutions using new graphene-based nanosorbents. *Chem. Eng. Trans.* **2015**, *45*, 1387−1392.
(20) Wang, X.; Deng, R.; Jin, X.; Huang, J. Gallic acid modified hyper-cross-linked resin and its adsorption equilibria and kinetics toward salicylic acid from aqueous solution. *Chem. Eng. J.* **2012**, *191*, 195−201.
(21) Wang, X.; Chen, L.; Liu, Y. N.; Huang, J. Macroporous crosslinked polydivinylbenzene/polyacryldiethylenetriamine (PDVB/PADETA) interpenetrating polymer networks (IPNs) and their efficient adsorption to o -aminobenzoic acid from aqueous solutions. *J. Colloid Interface Sci.* **2014**, *429*, 83−87.
(22) Fu, Z.; He, C.; Li, H.; Yan, C.; Chen, L.; Huang, J.; Liu, Y. N. A novel hydrophilic−hydrophobic magnetic interpenetrating polymer networks (IPNs) and its adsorption towards salicylic acid from aqueous solution. *Chem. Eng. J.* **2015**, *279*, 250−257.
(23) Wang, X.; Li, G.; Guo, D.; Zhang, Y.; Huang, J. A novel polar-modified post-cross-linked resin and its enhanced adsorption to salicylic acid: Equilibrium, kinetics and breakthrough studies. *J. Colloid Interface Sci.* **2016**, *470*, 1−9.
(24) Fu, Z.; Li, H.; Yang, L.; Yuan, H.; Jiao, Z.; Chen, L.; Huang, J.; Liu, Y. N. Magnetic polar post-cross-linked resin and its adsorption towards salicylic acid from aqueous solution. *Chem. Eng. J.* **2015**, *273*, 240−246.
(25) Arshadi, M.; Mousavinia, F.; Amiri, M. J.; Faraji, A. R. Adsorption of methyl orange and salicylic acid on a nano-transition metal composite: Kinetics, thermodynamic and electrochemical studies. *J. Colloid Interface Sci.* **2016**, *483*, 118−131.
(26) Tatarchuk, T.; Naushad, M.; Tomaszewska, J.; Kosobucki, P.; Cigalski, P. Adsorption of Sr(II) ions and salicylic acid onto magnetic magnesium-zinc ferrites: isotherms and kinetic studies. *Environ. Sci. Pollut. Res.* **2020**, *27*, 26681−26693.
(27) Karimi, M.; Rodrigues, A. E.; Silva, J. Designing a simple volumetric apparatus for measuring gas adsorption equilibria and kinetics of sorption. Application and validation for CO2, CH4 and N2 adsorption in binder-free beads of 4A zeolite. *Chem. Eng. J.* **2021**, *425*, 130538.
(28) Song, M.; Jiao, P.; Qin, T.; Jiang, K.; Zhou, J.; Zhuang, W.; Chen, Y.; Liu, D.; Zhu, C.; Chen, X.; et al. Recovery of Lactic Acid from the Pretreated Fermentation Broth Based on a Novel Hyper-Cross-Linked Meso-Micropore Resin: Modeling. *Bioresour. Technol.* **2017**, *241*, 593−602.
(29) Ko, D. C. K.; Porter, J. F.; McKay, G. Application of the concentration-dependent surface diffusion model on the multi-component fixed-bed adsorption systems. *Chem. Eng. Sci.* **2005**, *60*, 5472−5479.
(30) Xiao, G.; Wen, R.; Wei, D.; Wu, D. Effects of the Steric Hindrance of Micropores in the Hyper-Cross-Linked Polymeric Adsorbent on the Adsorption of p-Nitroaniline in Aqueous Solution. *J. Hazard. Mater.* **2014**, *280*, 97−103.
(31) Wang, W.; Qi, M.; Jia, X.; Jin, J.; Li, A. Differential adsorption of zwitterionic PPCPs by multifunctional resins: The influence of the hydrophobicity and electrostatic potential of PPCPs. *Chemosphere* **2020**, *241*, 125023.
(32) Zhang, T.; Huang, J. N -vinylimidazole modified hyper-cross-linked resins and their adsorption toward Rhodamine B: Effect of the cross-linking degree. *J. Taiwan Inst. Chem. Eng.* **2017**, *80*, 293−300.
(33) Schmidt-Traub, H.*Preparative Chromatography of Fine Chemicals and Pharmaceutical Agents*; Wiley-VCH, 2005.
(34) Jiao, P.; Wei, Y.; Zhang, M.; Zhang, X.; Yuan, X. Adsorption separation of L-tryptophan based on the hyper-cross-linked resin XDA-200. *ACS Omega* **2021**, *6*, 2255−2263.
(35) Babazadeh, M.; Abolghasemi, H.; Esmaeili, M.; Ehsani, A.; Badiei, A. Comprehensive batch and continuous methyl orange removal studies using surfactant modified chitosan-clinoptilolite composite. *Sep. Purif. Technol.* **2021**, *267*, 118601.
(36) Weber, W. J.; Morris, J. C. Kinetics of adsorption on carbon from solution. *J. Sanit. Eng. Div., Am. Soc. Civ. Eng.* **1963**, *89*, 31−59.
(37) Ren, T.*Study on Transport and Separation of Aromatic Acids and Phenol by Polymer Inclusion Membrane*; Xi'an University of Architecture and Technology: Xi'an, 2019.
(38) Zheng, J.; He, X.; Cai, C.; Xiao, J.; Liu, Y.; Chen, Z.; Pan, B.; Lin, X. Adsorption isotherm, kinetics simulation and breakthrough analysis of 5-hydroxymethylfurfural adsorption/desorption behavior of a novel polar-modified post-cross-linked poly (divinylbenzene-co-ethyleneglycoldimethacrylate) resin. *Chemosphere* **2020**, *239*, 124732.
(39) Volkov, N. A.; Tuzov, N. V.; Shchekin, A. K. Molecular dynamics study of salt influence on transport and structural properties of SDS micellar solutions. *Fluid Phase Equilib.* **2016**, *424*, 114−121.
(40) Harned, H. S.; Nuttall, R. L. The diffusion coefficient of potassium chloride in dilute aqueous solution. *J. Am. Chem. Soc.* **1947**, *69*, 736−740.
(41) Wilke, C. R.; Chang, P. Correlation of Diffusion Coefficients in Dilute Solutions. *AIChE J.* **1955**, *1*, 264−270.

https://doi.org/10.1021/acsomega.2c04892
ACS Omega 2022, 7, 36679−36688